Surface electronic inhomogeneity of the (001)-SrTiO3:Nb crystal with a terrace-structured morphology

Y. Li, J. R. Sun, J. L. Zhao, and B. G. Shen

Citation: J. Appl. Phys. **114**, 154303 (2013); doi: 10.1063/1.4825047
View online: http://dx.doi.org/10.1063/1.4825047
View Table of Contents: http://jap.aip.org/resource/1/JAPIAU/v114/i15
Published by the AIP Publishing LLC.

Surface electronic inhomogeneity of the (001)-$SrTiO_3$:Nb crystal with a terrace-structured morphology

Y. Li, J. R. Sun,[a] J. L. Zhao, and B. G. Shen
Beijing National Laboratory for Condensed Matter Physics and Institute of Physics, Chinese Academy of Sciences, Beijing 100190, China

(Received 21 May 2013; accepted 27 September 2013; published online 15 October 2013)

Local surface conduction of the (001)-orientated $SrTiO_3$:Nb crystal with a terrace-structured morphology has been studied by means of conductive atomic force microscope analysis. We found that the surface conductance is inhomogeneous on the atomic scale; it is high near step edges and low on terrace plateaus. The surface conductance fluctuation is susceptible to post annealing, first enhancing and then weakening while repeatedly annealed at 700 °C in vacuum. Considering the fact that the oxygen content is most sensitive to vacuum annealing for the temperatures adopted here, the inhomogeneous conductance implies the difference of oxygen vacancy content at step edges and terrace plateaus. The present work clearly demonstrated the influence of surface microstructure on physical properties, and could be helpful for the understanding of the atomic scale non-uniformity of the ultrathin films fabricated on step-featured $SrTiO_3$ surface.
 [http://dx.doi.org/10.1063/1.4825047]

I. INTRODUCTION

$SrTiO_3$ (STO) is an important perovskite oxide which has been extensively studied due to its versatile physical properties. It was known as a material with high dielectric constant. However, when doped with a small amount of Nb or oxygen vacancies, it transits from a wide-bandgap semiconductor into a high-mobility metal or even a superconductor.[1,2] It also exhibits a special capability in accommodating oxygen vacancies. Instead of evenly distributing in the interior of bulk STO, oxygen vacancies prefer to diffuse towards surface, yielding a concentration gradient from surface to interior.[3]

In addition to these, STO is also a promising substrate due to its compatible lattice parameters with most perovskite oxides and chemical stability, and has been widely used in the growth of, for example, superconducting, colossal magnetoresistive, and multiferroic thin films. A distinctive character of the STO crystal is particularly favourable, i.e., the formation of terrace-like structure on (001) surface after chemical etching and subsequent high temperature annealing.[4,5] This feature favors a layer by layer film growth, a growth mode for high quality thin films. It can also be used to modify the physical properties of the above film, especially ultrathin films with behaviors strongly depending on interface. Besides interface strains, the surface structures of the substrate such as surface step, terrace, kink sites as well as other defect distribution are also important factors affecting the physical properties of the films.[6–11] Anisotropic planar defects and transport properties originating from substrate step edges were indeed observed in oxide superconductor thin films.[7–9] For the two-dimensional electron gas at the STO-$LaAlO_3$ (LAO) interface, it was lately found that the electron mobility is different along and perpendicular to the terrace edges of the surface.[10] Recent experiments also revealed a non-uniform distribution of metallic and insulating domains on the step-structured surface of the $(La_{0.4}Pr_{0.6})_{0.67}Ca_{0.33}MnO_3$ film, and terrace steps confine one dimension of the metallic domains remarkably.[11] These works clearly demonstrated the important effects of the substrate surface on ultrathin films. Therefore, a thorough investigation of the surface properties of the substrate is worthwhile for the designing and understanding of artificial materials and corresponding emergent phenomena.[12–14]

In fact, the effect of surface steps has been studied for metal surfaces both theoretically and experimentally, and there is clear evidence for the occurrence of remarkable inhomogeneous physical properties.[15,16] For the STO (insulator) surface with steps, there are a large number of reports on structure reconstructions,[5,17–21] but scarce on local physical properties. In this paper, we observed inhomogeneous conduction on Nb-doped STO substrate with terrace-structured morphology by means of conductive atomic force microscope (C-AFM) analysis.[22] It is found that the surface conductance is high at step edges and low on terrace plateaus. Annealing the sample in vacuum modified the inhomogeneity in the meantime enhancing the overall conductance, which is a signature of different release rates for the oxygen atoms at different locations of the sample surface.

II. EXPERIMENTS

Commercial (001)-orientated 0.05 wt. % Nb-doped $SrTiO_3$ (STON05) crystal with one polished side (3×1 mm^2) was carefully cleaned by ultrasonic washing in acetone and alcohol in sequence without chemical treatment. To remove possible surface contaminations, the sample was treated at 200 °C for 1 h in a vacuum of 10^{-4} Pa. The temperature was so chosen that it can remove the sticking adsorbates without affecting the oxygen content of STON05. The sample thus obtained will be denoted as "as-cleaned" hereafter. To get a

[a]Author to whom correspondence should be addressed. Electronic mail: jrsun@iphy.ac.cn

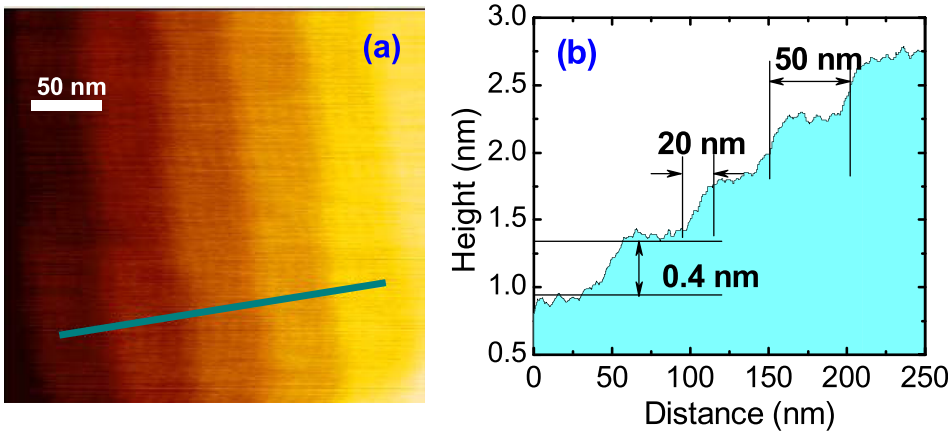

FIG. 1. Surface morphology of (001)-orientated STON05 (a) and the corresponding line profile along the line marked in the topology image (b). The line is perpendicular to the terrace edge.

definite TiO_2 terminated layer, a 0.8 wt. % Nb-doped $SrTiO_3$ (STON8) crystal was prepared by chemical etching in buffered HCl and subsequent annealing at 900 °C in O_2 flow. The resulted step height is either 2 or 3 unit cells. According to our experiments, a higher temperature usually leads to higher steps.[23] The step edge is sharp and the terrace plateau is flat, well suitable for the present study. Here, we selected a crystal with a considerably high Nb content to guarantee considerable surface conductance after the annealing in O_2 atmosphere. The local conduction was studied by C-AFM, adopting a Pt-coated tip with a curvature radius of ~20 nm and a spring constant of ~14 N/m. During the experiments, the tip was grounded, and the sample was biased by U_{sample}. The sample was connected to sample holder by silver paste. Appropriate electric pulses were applied to the Ag-STON contact to get an Ohmic contact. For the convenience of data analysis, we denote the voltage drop from the tip to the sample as $U_{tip} = -U_{sample}$. All experiments were conducted in vacuum at ambient temperature. Topography and spatial current distribution were measured simultaneously.

III. RESULTS AND DISCUSSIONS

The as-cleaned sample was first studied. Fig. 1(a) shows the topography of STON05. Like in other works,[24] the C-AFM analysis requires a metal-coated tip, and this usually lowers the spatial resolution of the topographic image. In spite of this, well organized terrace structure can still be identified. As shown by the line profile in Fig. 1(b), the step height is ~0.4 nm, which is exactly the height of one unit cell of STO, and the distance between adjacent terrace steps is ~50 nm. The terrace width is much greater than the curvature radius of the tip (~20 nm), thus allows the acquirements of current distribution with a high spatial resolution.

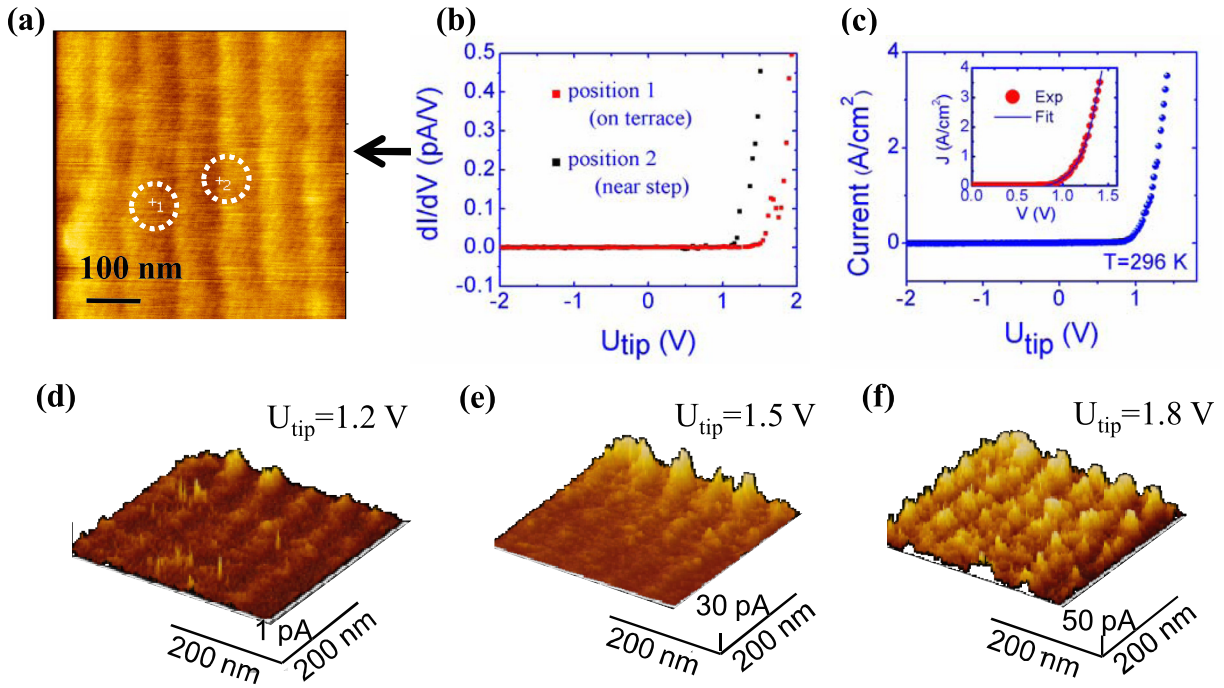

FIG. 2. C-AFM images of the morphology (a) and change of current vs tip potential (dI/dU vs U_{tip}) near steps and on terraces (b) for STON05. Typical current-voltage characteristic in linear scale near steps (c) and the corresponding current mappings recorded under the biases of 1.2 V (d), 1.5 V (e), and 1.8 V (f) (For a U_{tip} below 1 V the current is below the detection limit of the C-AFM system). The inset solid line shows the result of curve-fitting based on the Shockley equation. The tip bias ($U_{tip} = -U_{sample}$) is defined as the voltage drop from the tip to the sample.

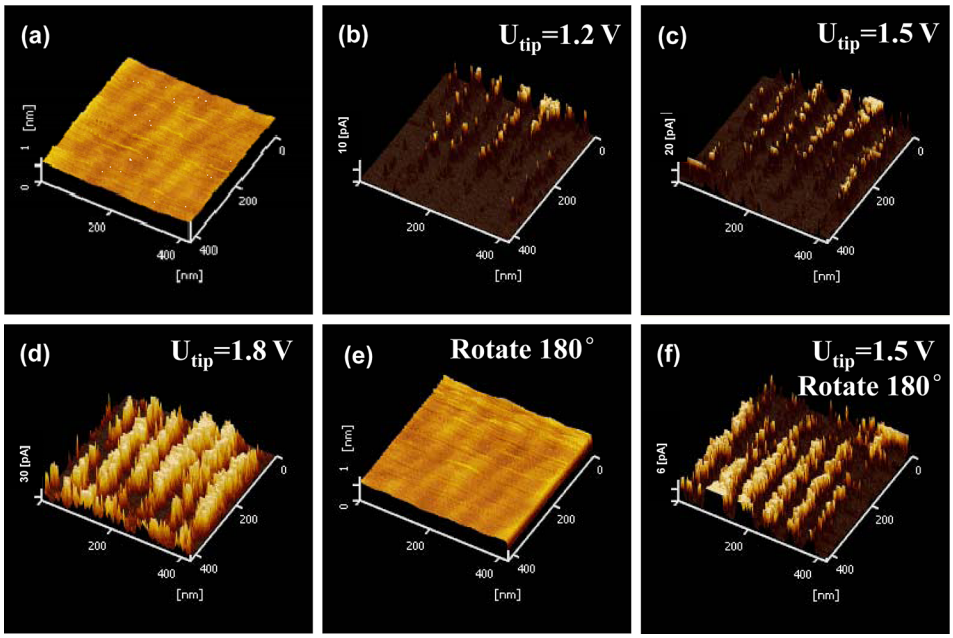

FIG. 3. Surface morphology of sample and corresponding current mappings for STON05, measured under $U_{tip} = 1.2$ V (b), 1.5 V (c), and 1.8 V (d). (e) and (f) are the morphology and spatial variation of current in the same location after rotating the sample by 180°.

Current-voltage (J–V) characteristics were measured for different representative locations near step edges and on terraces (Figs. 2(a) and 2(b)). The dI/dU vs U_{tip} curves show significant difference, and step edges are more conducting than terrace plateaus. We have analysed the typical J–V curves near steps (inset in Fig. 2(c)). The anisotropic dependence of current on electric polarity indicates the presence of an interfacial barrier at the Pt–STON contact. The J–V relation can be well described by the Shockley equation $J = J_s \exp(eV/nk_BT)\text{-}J_1$ (solid line in Fig. 2(c)), where $J_s = AT^2 \exp(-\Phi_B/k_BT)$ is the saturation current, n is the ideality factor, k_B is the Boltzmann constant, and J_1 is a parameter describing zero point shift. The non-zero current J_1 in our data is very small compared with thermionic current J_s, and will not affect our analysis. The deduced ideality factor is ~6.4, much greater than unity. It suggests the presence of interfacial states. The Schottky barrier can also be determined, and it is $\Phi_B \approx 0.6$ eV adopting the junction area of $\sim 1.2 \times 10^3$ nm^2 (the effective area of the tip). The electron affinity of STO is 3.9 eV and the work function of Pt is 5.6 eV. The expected barrier height for the Pt-STO contact is ~1.7 eV, much larger than that deduced. Under positive biases ($U_{tip} > 0$), the charge transport through the Pt-STON contact may proceed via both thermionic emission and thermally assisted electron tunneling when the carrier concentration in STON05 is high. The latter process usually causes an underestimated interfacial barrier and an overestimated ideality factor.

According to Fig. 2(c), the current shows a crucial dependence on forward bias when $U_{tip} > 0.8$ V, and any variations in surface state could be susceptibly sensed by the J–V curves. To get the information about surface state, the spatial current distribution has been acquired under several typical U_{tip} above 0.8 V. Figs. 2(d)–2(f) present the 3-dimensional plots of current distribution recorded under 1.2 V, 1.5 V, and 1.8 V, respectively. As bias grows, prominent current peaks emerge at more and more locations, forming parallel ridges with a separation of ~50 nm (Fig. 2(f)). This phenomenon is not accidental, and has been observed in different regions of sample surface (Fig. 3). The scanning direction of the tip was from left to right for the above measurements. However, rotating the sample by 180° (equivalent to a right to left scanning), we observed similar phenomenon (Fig. 3(f)). So the current fluctuation cannnot be ascribed to the different contact of the tip apex and tip side with surface steps. Also, we replaced the Pt tip by Au-coated and Rh-coated tips, and found that the regular current distribution remains existed (not shown). All these indicate that the surface inhomogeneity in STON05 is not an artifact.[25]

It is instructive to compare Figs. 1 and 2. The ridge-shaped structure is a common feature of the surface morphology and current mapping. It implies a correspondence between microstructure and current distribution. This inference is quantitatively confirmed by the data in Fig. 4, where line profiles of surface morphology and current distribution are compared. Figs. 4(a) and 4(b) are, respectively, the plane views of the surface morphology and current mapping, obtained under the bias of $U_{tip} = 1.5$ V. Fig. 4(c) is the corresponding line profiles along the lines marked in Figs. 4(a) and 4(b). The correspondence between current peak and step edge is evident; the former appears at regions where the latter locates. On average, the current is above ~20 pA near step edge and ~7 pA on terrace plateau. The average peak width (full width at half maximum) is ~23 nm, which is very similar to the step width of the terrace (~20 nm). The step heights in all scanned areas are the same (~0.4 nm). This implies that sample STON05 has a definite termination, which may be TiO_2 as franchiser declared. To clarify the effect of termination layer, the local conduction of STON8, which owns a TiO_2 termination but slightly higher steps (~2–3 unit cells), is further studied. As expected, the strong surface structure-conduction correlation is also observed (Figs. 4(g)–4(i)). The step height of STON8 is ~2–3 unit cells, rather than 1 unit cell. Although the step height is slightly different for samples STON05 and STON8, fascinatingly, the local conduction exhibits exactly the same features

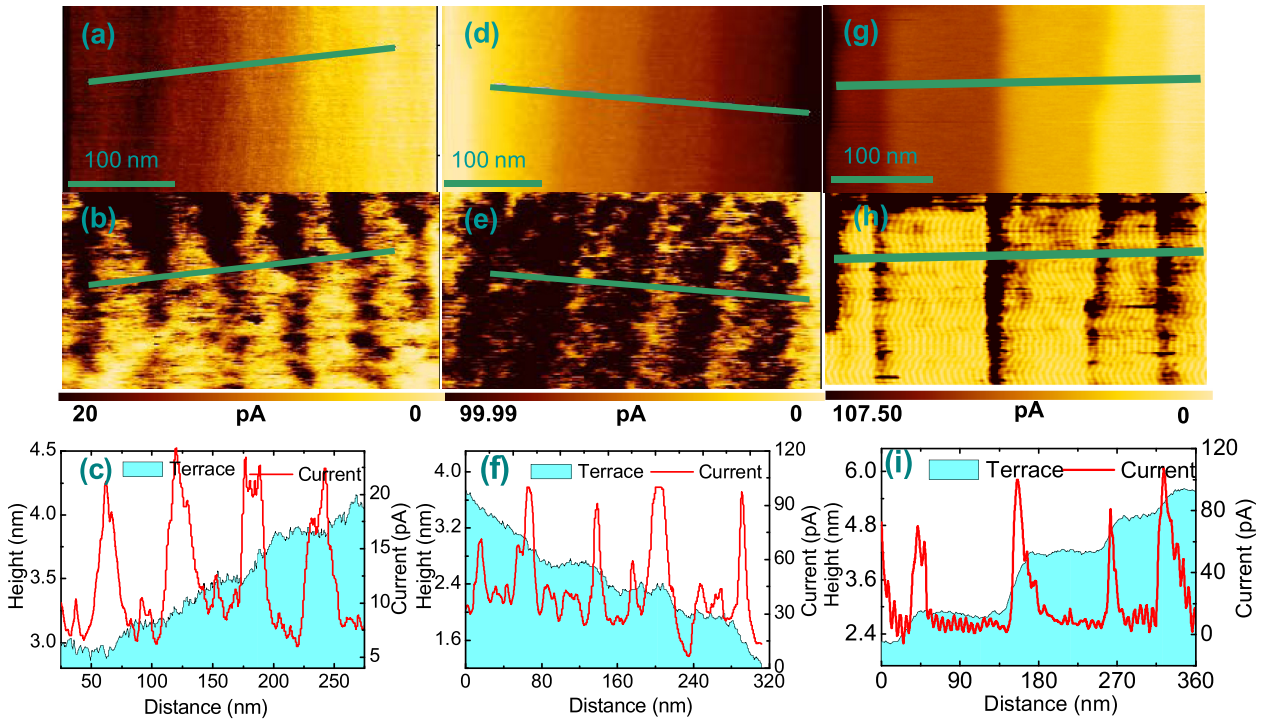

FIG. 4. Surface morphology of the as-cleaned and first annealed STON05 ((a) and (d)) and corresponding current mappings under $U_{tip} = 1.5$ V ((b) and (e)). (c) and (f) are line profiles of surface structure and spatial current distribution for as-cleaned and first annealed STON05, respectively. The corresponding data for STON8 were presented in (g), (h), and (i). Dark areas represent high current values. The decrease in current peak in the lower part of the image in (b) could be a consequence of tip pollution due to impurity adherence.

(Figs. 4(g)–4(i)). These results confirm the occurrence of inhomogeneous surface conduction.

To get a general idea about the electrical inhomogeneity, in Fig. 5 we show the spatial distribution of the current along the direction perpendicular to step edge ($U_{tip} = 1.5$ V). To depress random fluctuation, data obtained here are averaged over the entire image. Although this process may smear out sharp changes, the main features of the current distribution remain unaffected. As shown in Fig. 5, current value displays a regular oscillation with position, and the low and high currents are ~6 pA and ~19 pA, respectively. These results clearly demonstrate the correlation between topography and surface conduction. Regular current oscillation is also observed in the images under other biases, and it is therefore a general feature of STON.

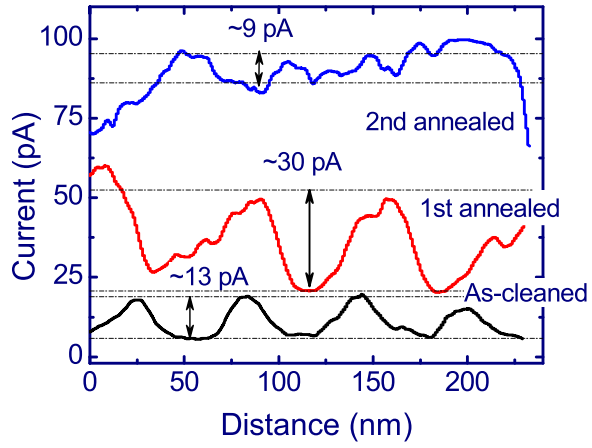

FIG. 5. Spatial variation of current recorded under a bias $U_{tip} = 1.5$ V for STON05. The labels "1st and 2nd annealed" refer to annealing at 700 °C for 30 and 45 min, respectively.

As reported, vacuum annealing at the temperature above 1000 K can lead to metallic behavior.[18] By annealing the sample in vacuum at high temperatures, one may affect the oxygen content on surface, and consequently surface conductance. In view of this, the morphology-current distribution correlation is further studied after annealing STON05 at 700 °C for 30 and 45 min, in sequence, in a vacuum environment of 10^{-4} Pa. As shown in Figs. 4(d)–4(f), the first vacuum annealing process has little influence on the microstructure of sample surface whereas enhances the electric nonuniformity of sample surface. As shown in Fig. 5, the peak and valley current values in the waved curve are ~22 pA and ~52 pA, respectively ($U_{tip} = 1.5$ V), i.e., the peak-to-valley amplitude is ~30 pA. The corresponding current increments, compared with the as-cleaned state, are ~15 pA and ~32 pA, respectively. The conductance of step edge changes more quickly than that of terrace plateau. Meanwhile, the overall surface conductance is enhanced; the average current is ~37 pA under the bias of 1.5 V, much larger than that of the as-cleaned sample (~13 pA). These results reveal an enhancement of surface inhomogeneity and overall conductance after the first annealing.

Defining, respectively, the peak and valley currents as I_{peak} and I_{valley}, in Fig. 6 we show the evolution of the relative current difference at step edge and terrace plateau with vacuum annealing $\delta = (I_{peak}\text{-}I_{valley})/I_{valley}$. δ is small at low biases, only ~0.27 at the forward-bias of 1.0 V. It undergoes an increase-to-decrease transition as tip bias sweeps through

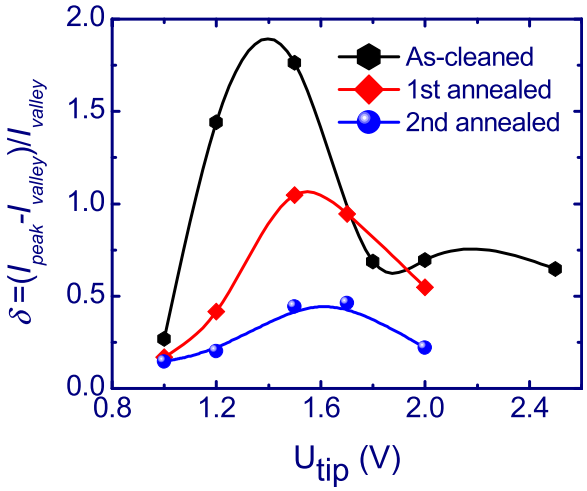

FIG. 6. Relative current difference at step edges and on terrace plateau, obtained under different tip biases.

~1.5 V. The maximal current difference is ~1.8, obtained under $U_{tip} = 1.5$ V, i.e., the current at step edge is nearly twice as large as that on terrace plateau. The maximal current difference, obtained under the forward bias of 1.5 V, is ~1.05 after the first annealing, and ~0.44 after the second annealing.

The inhomogeneous current distribution implies different surface states at the terrace step and plateau. Considering the different local environments for the atoms at step edges and on terrace plateaus, we propose the occurrence of different structure re-constructions at step edges and on terrace plateaus in the process of mechanical polishing or chemical etching plus post-annealing. This leads to a spatial distribution of the Pt-STON interfacial barrier,[26] causing the inhomogeneous electronic transport through the Pt-STON contact. As reported, the main effect produced by a vacuum annealing at 700 °C is the deflection of oxygen content from stoichiometry in STO.[18,27] It is possible that the content of oxygen vacancies is different at step edges and terrace plateaus, due to the different local environments for the oxygen atoms at these two kinds of locations, and this may be the underlying reason for the inhomogeneous surface conductance. As well known, the presence of oxygen vacancies favors the electron tunneling through the Pt-STON contact, thus enhances surface conduction. Step edges may be preferred locations for oxygen vacancies, therefore exhibit a high conductance. This inference is consistent with the observations that the conductance of the step edges increases more rapidly than that of terrace plateaus after vacuum annealing. However, over-annealing may depress the edge-plateau difference since the oxygen release at step edges will be slowed down when the oxygen content there is much lower than that of the plateau. This explains the results of the second annealing. As shown in Fig. 5, the spatial current variation is significantly depressed by the second annealing of 45 min. Although slight current fluctuation can still be seen, its spatial variation is relatively irregular, and its correlation to terrace structure disappears.

The bias dependence of δ is understandable noting the crucial dependence of conduction on U_{tip} in Fig. 2(c). According to Fig. 2(c), there is a threshold voltage for the current lifting in the J–V curve (~1 V). When voltage bias varies in a range near the threshold voltage, the current may grow at different speeds at step edges and on terrace plateaus. This actually implies a variation of (I_{peak}-I_{valley}) with U_{tip}. When U_{tip} well exceeds the threshold voltage, however, both the step edge and the terrace plateau are in a high conduction state, and the current difference diminishes.

Alternatively, the inhomogeneous conductions can also be ascribed to the difference of the surface layers at step edge and plateau. As shown by Fig. 1, the surface layers of the terrace plateau and step edge are different, i.e., if the terminated layer is TiO_2, the atoms in the middle of the step edge will be SrO and vice verse. Annealing at higher temperatures will gradually diminish the amount of SrO and result in surface segregation and bulk diffusion of niobium or strontium atoms. This process may undergo unevenly at terrace edge and plateau, resulting in the regular evolution of inhomogeneous surface conduction. Previous studies have demonstrated the importance of these contributions for various annealing processes.[28–30]

The vicinal angle of surface of STON05 is ~0.4° and STON8 is 0.6°. Vicinal angle will influence surface homogeneity by affecting terrace width, thus the density of the steps on sample surface.

IV. SUMMARY

Surface conduction of the (001)-STON crystal with terrace-structured morphology has been studied by means of C-AFM analysis. Inhomogeneous current distribution is detected under a fixed tip bias. The current is high near step edges and low on terrace plateaus, indicating a strong correlation between surface conduction and surface structure. Appropriate post annealing in vacuum can considerably intensify the conductive difference in the meantime enhancing the overall conductance. Based on the analysis of the experimental results, we proposed that the oxygen content is different at step edges and terrace plateaus due to the different local environments at these two kinds of locations, and this is the origin for inhomogeneous conductance. This characteristic of the STON substrate is expected to influence the ultrathin films grown on it, providing an approach towards an effective tailoring of the physical properties of perovskite thin films.

ACKNOWLEDGMENTS

This work has been supported by the National Basic Research of China, the National Natural Science Foundation of China, the Knowledge Innovation Project of the Chinese Academy of Science, and the Beijing Municipal Nature Science Foundation.

[1]H. Yamada and G. R. Miller, J. Solid State Chem. **6**, 169 (1973).
[2]E. R. Pfeiffer and J. F. Schooley, Phys. Lett. A **29**, 589 (1969).
[3]Z. Q. Liu, D. P. Leusink, X. Wang, W. M. Lǔ, K. Gopinadhan, A. Annadi, Y. L. Zhao, X. H. Huang, S. W. Zeng, Z. Huang, A. Srivastava, S. Dhar, T. Venkatesan, and Ariando, Phys. Rev. Lett. **107**, 146802 (2011).

[4]M. Kawasaki, A. Ohtomo, T. Arakane, K. Takahashi, M. Yoshimoto, and H. Koinuma, Appl. Surf. Sci. **107**, 102 (1996).
[5]J. Zegenhagen, T. Haage, and Q. D. Jiang, Appl. Phys. A **67**, 711 (1998).
[6]D. X. Huang, C. L. Chen, and A. J. Jacobson, J. Appl. Phys. **97**, 043506 (2005).
[7]J. Fujita, T. Yoshitake, T. Satoh, S. Miura, H. Tsuge, and H. Igarashi, Appl. Phys. Lett. **59**, 2445 (1991).
[8]J. S. Tsai, J. Fujita, and M. Yu. Kupriyanov, Phys. Rev. B **51**, 16267 (1995).
[9]A. Ogawa, T. Sugano, H. Wakana, A. Kamitani, S. Adachi, Y. Tarutani, and K. Tanabe, J. Appl. Phys. **97**, 013903 (2005).
[10]P. Brinks, W. Siemons, J. E. Kleibeuker, G. Koster, G. Rijnders, and M. Huijben, Appl. Phys. Lett. **98**, 242904 (2011).
[11]S. Singh, M. R. Fitzsimmons, H. Jeen, A. Biswas, and M. E. Hawley, Appl. Phys. Lett. **101**, 022404 (2012).
[12]R. V. Chopdekar, E. Arenholz, and Y. Suzuki, Phys. Rev. B **79**, 104417 (2009).
[13]Y. Segal, K. F. Garrity, C. A. F. Vaz, J. D. Hoffman, F. J. Walker, S. Ismail-Beigi, and C. H. Ahn, Phys. Rev. Lett. **107**, 105501 (2011).
[14]W. W. Gao, X. Sun, B. G. Shen, and J. R. Sun, J. Phys. D: Appl. Phys. **44**, 025002 (2011).
[15]J. Y. Park, G. M. Sacha, M. Enachescu, D. F. Ogletree, R. A. Ribeiro, P. C. Canfield, C. J. Jenks, P. A. Thiel, J. J. Saenz, and M. Salmeron, Phys. Rev. Lett. **95**, 136802 (2005).
[16]I. Merrick, J. E. Inglesfield, and G. A. Attard, Phys. Rev. B **71**, 085407 (2005).
[17]P. A. W. van der Heide, Q. D. Jiang, Y. S. Kim, and J. W. Rabalais, Surf. Sci. **473**, 59 (2001).
[18]V. E. Henrich, G. Dresselhaus, and H. J. Zeiger, Phys. Rev. B **17**, 4908 (1978).
[19]D. M. Kienzle, A. E. Becerra-Toledo, and L. D. Marks, Phys. Rev. Lett. **106**, 176102 (2011).
[20]T. Kubo and H. Nozoye, Surf. Sci. **542**, 177 (2003).
[21]M. R. Castell, Surf. Sci. **505**, 1 (2002).
[22]J. Y. Park, S. Maier, B. Hendriksen, and M. Salmeron, Mater. Today **13**(10), 38 (2010).
[23]Repeated experiments showed that the annealing temperature required by Nb-STO is lower than that by $SrTiO_3$, which is generally ~1000 °C.
[24]I. C. Infante, F. Sanchez, and J. Fontcuberta, J. Appl. Phys. **101**, 093902 (2007).
[25]Although the termination of STON05, SrO, or TiO_2 cannot be identified based on morphology analysis, the uniform step height indicates the invariance of the terminated layer across the area scanned. Therefore, the conductance at different location of the sample surface is comparable.
[26]T. Shimizu and H. Okushi, J. Appl. Phys. **85**, 7244 (1999).
[27]T. Matsumoto, H. Tanaka, T. Kawai, and S. Kawai, Surf. Sci. **278**, L153 (1992).
[28]R. Moos and K. H. Haerdtl, J. Am. Ceram. Soc. **80**, 2549 (1997).
[29]R. Meyer, R. Waser, J. Helmbold, and G. Borchardt, J. Electroceram. **9**, 101 (2002).
[30]E. Arveux, S. Payana, M. Maglionea, and A. Klein, Appl. Surf. Sci. **256**, 6228 (2010).